

NASA Contractor Report 178178

ICASE REPORT NO. 86-57

ICASE

SOME RECENT DEVELOPMENTS IN SPECTRAL METHODS

M. Y. Hussaini

(NASA-CR-178178) SOME RECENT DEVELOPMENTS
IN SPECTRAL METHODS Final Report (NASA)
20 p CSCL 20D

N87-11127

Unclas

G3/34 43964

Contract Nos. NAS1-17070, NAS1-18107

August 1986

INSTITUTE FOR COMPUTER APPLICATIONS IN SCIENCE AND ENGINEERING
NASA Langley Research Center, Hampton, Virginia 23665

Operated by the Universities Space Research Association

NASA

National Aeronautics and
Space Administration

Langley Research Center
Hampton, Virginia 23665

SOME RECENT DEVELOPMENTS IN SPECTRAL METHODS

M. Y. Hussaini

Institute for Computer Applications in Science and Engineering

ABSTRACT

This paper is solely devoted to spectral iterative methods including spectral multigrid methods. These techniques are explained with reference to simple model problems. Some Navier-Stokes algorithms based on these techniques are mentioned. Results on transition simulation using these algorithms are presented.

The research for the author was supported under the National Aeronautics and Space Administration under NASA Contract Nos. NAS1-17070 and NAS1-18107 while in residence at ICASE, NASA Langley Research Center, Hampton, VA 23665.

SOME RECENT DEVELOPMENTS IN SPECTRAL METHODS

M. Y. Hussaini

ICASE

NASA Langley Research Center

Hampton, VA 23665

1. Introduction

Spectral methods consist of expanding the solution to a problem in terms of basis functions which are global, infinitely differentiable and preferably orthogonal [1,2]. This choice of basis functions is what distinguishes them from the finite difference and finite element methods. In the case of finite element methods, the domain is divided into small elements, and a basis function is specified in each element. They are thus local in character. The case with finite difference methods is similar.

In addition to the basis functions, a key element of spectral methods is the set of test functions or weight functions. The test functions are used to enforce minimization of the residual resulting from the substitution of the series expansion of the solution into the differential equation. The choice of test functions distinguishes between essentially two types of spectral methods – spectral Galerkin, and spectral collocation. In the Galerkin approach, the test functions are usually the same as the basis functions, whereas in the collocation approach the test functions are translated Dirac delta functions. In other words, the Galerkin approach satisfies the differential equations in the least square sense. In the spectral collocation approach the equations are satisfied exactly at the selected, so-called collocation points. It should be noted that the basis functions are employed solely for the purpose of approximating derivatives. This approach, which became feasible with the advent of computers, is the easiest and the most efficient for nonlinear problems, and is the focus of the present discussion.

2. Basic Aspects

The principal advantage of spectral methods lies in their potential for rapidly convergent approximations. In practical terms, it means that they achieve accurate results with substantially fewer points than are required by typical finite difference methods. Suppose u_N is a numerical approximation to a function $u(x)$. With a given set of basis functions Φ_n , it takes the form

$$u_N(x) = \sum_{n=0}^N a_n \Phi_n(x). \quad (1)$$

The expansion coefficients a_n are obtained by enforcing the condition

$$u_N(x_j) = u(x_j). \quad (2)$$

where x_j are the selected, so-called collocation points, which are usually the extrema of Φ_N . Figure 1 provides a graphic distinction between a second-order accurate central difference approximation and a Legendre spectral approximation to the first derivative of the function

$$u(x) = 1 + \sin(2\pi x + \frac{\pi}{4}) \quad \text{on } [-1, 1]$$

whose values are given at a finite number of grid points. The finite difference approximation for the derivative at the origin, for instance, is estimated by interpolating a parabola through the origin and the two adjacent points, and is thus local in character. The spectral approximation estimates the derivative of the original function by the derivative of the polynomial which interpolates all the available points. Note that the error of the finite difference discretization decreases as $1/N^2$, whereas the error of the spectral discretization decreases exponentially. In the case of a differential equation, a further step is involved, that of finding an approximation for the differential operator in terms of the grid point values $u_N(x_j)$.

Another advantage of spectral methods is their minimal phase error. Consider the periodic solution to the problem $u_t + u_x = 0$ with $u(x,0) = \sin(\pi \cos(x))$. Figure 2 shows the lagging phase of the finite difference solution, while the Fourier spectral solution has zero phase error. A fourth-order Runge-Kutta method is used for temporal discretization in both the cases. For realistic problems with variable coefficients or nonlinear terms, the phase error for spectral methods is, of course, nonzero, but still relatively small.

These are some of the essential aspects of spectral methods which make them the prevailing tool in the study of stability, transition, and turbulence. Some of the drawbacks which have inhibited their wider use are: 1) time-step restriction imposed by the standard spectral grid, 2) sensitivity to singularities and 3) restriction to simple geometry. Progress has been made on all counts [3]. The present work will be confined to the recent developments in overcoming the first obstacle.

3. Iterative Spectral Methods

For evolution problems, explicit time-stepping can be extremely inefficient. This is so because the typical time-step limitation for spectral methods is proportional to $1/N^2$ for the advection equation and $1/N^4$ for the diffusion equation (where N is the number of modes) [1]. Hence, implicit time-stepping becomes a necessity. This results in a set of algebraic equations, which are in general amenable to iterative solution techniques only. Also, elliptic equations governing practical problems virtually require implicit iterative techniques. As the condition number of the relevant matrices are large, preconditioned iterative schemes including multigrid procedures are the attractive choices. In this section, we discuss the fundamentals of iterative spectral methods with reference to an elementary example, and then their application to the three dimensional incompressible Navier Stokes equations for the study of stability and transition in a channel and a boundary layer.

For the purpose of illustration let us consider the equation,

$$u_x = f, \quad (3)$$

periodic on $[0, 2\pi]$. For the Fourier method, the standard choice of collocation points is

$$x_j = \frac{2\pi j}{N}, \quad j = 0, 1, 2, \dots, N-1, \quad (4)$$

Setting $u_j = u(x_j)$, the discrete Fourier series for u may be represented by the discrete transform pair

$$u_j = \sum_{p=-\frac{N}{2}}^{\frac{N}{2}-1} \hat{u}_p e^{ipx_j} \quad j = 0, 1, \dots, N-1$$

$$\hat{u}_p = \frac{1}{N} \sum_{j=0}^{N-1} u_j e^{-ipx_j}, \quad p = -\frac{N}{2}, \dots, \frac{N}{2}-1$$

The expression for the derivative u_x at the collocation points is

$$u_x(x_j) = \sum_{p=-\frac{N}{2}+1}^{\frac{N}{2}-1} ip \hat{u}_p e^{ipx_j}, \quad j = 0, 1, \dots, N-1$$

Thus the Fourier collocation discretization of the equation may be written

$$LU = F, \quad (5)$$

where $U = (u_0, u_1, \dots, u_{N-1})$, $F = (f_0, f_1, \dots, f_{N-1})$, and $L = C^{-1}DC$ with C being the discrete Fourier transform operator, C^{-1} the inverse transform, and D the diagonal matrix denoting the first derivative operator in the Fourier space. Specifically,

$$C_{jk} = e^{-2\pi i k \frac{(j-N/2)}{N}}, \quad j, k = 0, 1, \dots, N-1 \quad (6)$$

and

$$\begin{aligned} D_{jj} &= i(j - N/2) && \text{for } j = 1, 2, \dots, N-1 \\ &= 0 && \text{for } j = 0 \end{aligned} \quad (7)$$

The eigenvalues of L are $\lambda(p) = ip$, $p = -N/2 + 1, \dots, N/2 - 1$, and the largest one grows as $N/2$. A preconditioned Richardson iterative procedure for solving Eq. (5) is

$$V \leftarrow V + \omega H^{-1} (F - LV) \quad (8)$$

where the preconditioning matrix H is an approximation to L , is sparse, and is readily invertible. An obvious choice for H is a finite difference approximation L_{FD} to the first derivative. With the various possibilities for L_{FD} , the eigenvalue spectrum of $L_{FD}^{-1}L$ is given in Table 1. Apparently, the staggered grid leads to the most effective treatment of the first derivative. This kind of preconditioning was successfully used in the semi-implicit time-stepping algorithm for the Navier Stokes equations discussed in the section on Navier Stokes Algorithms. The eigenvalue trends of that complicated set of vector equations are surprisingly well predicted by this extremely simple scalar periodic problem.

Next, let us consider the second order equation

$$-u_{xx} = f \quad \text{on } [0, 2\pi] \quad (9)$$

with periodic boundary conditions. A Fourier collocation discretization of this equation is the same as Eq. (5) except for the diagonal matrix D which represents now the second derivative operator in the Fourier space.

$$D_{jj} = -\left(j - \frac{N}{2}\right)^2, \quad j = 1, 2, \dots, N-1$$

$$= 0, \quad j = 0$$

The eigenvalues of L are $\lambda(p) = p^2$, $p = -N/2 + 1, \dots, N/2 - 1$. To make the case for the multigrid procedure (consisting of a fine-grid operator and a coarse-grid correction) as a preconditioner, we assume H to be the identity matrix I in the iterative scheme (8). The iterative scheme is convergent if the eigenvalues, $(1 - \omega\lambda)$, of the iteration matrix $[I - \omega L]$ satisfy

$$|1 - \omega\lambda| < 1.$$

Each iteration damps the error component corresponding to λ by a factor $v(\lambda) = |1 - \omega\lambda|$. The optimal choice of λ is that which balances damping of the lowest-frequency and the highest-frequency errors, i.e.,

$$(1 - \omega\lambda_{\max}) = -(1 - \omega\lambda_{\min})$$

This yields

$$\omega_{SG} = \frac{2}{(\lambda_{\max} + \lambda_{\min})},$$

and the spectral radius

$$\mu_{SG} = \frac{(\lambda_{\max} - \lambda_{\min})}{(\lambda_{\max} + \lambda_{\min})}.$$

In the present instance, $\lambda_{\max} = N^2/4$, $\lambda_{\min} = 1$, and thus $\mu_{SG} = 1 - 8/N^2$. This implies order N^2 iterations are needed for convergence. This poor performance is due to balancing the damping of the lowest frequency eigenfunction with the highest-frequency one. The multigrid procedure exploits the fact that the lowest-frequency modes ($|p| < N/4$) can be damped efficiently on coarser grids, and settles for a relaxation parameter value which balances the damping of the mid-frequency mode ($|p| = N/4$) with the highest-frequency one ($|p| = N/2$). Table 2 provides the comparison of single-grid and multigrid damping factors for $N=64$. The high frequencies from 16 to 32 are damped effectively in the multigrid procedure, whereas the frequencies lower than 16 are hardly damped at all. But then some of these low frequencies (from 8 to 16) can be efficiently damped on the coarser grid with $N=32$. Further coarser grids can be employed till relaxation becomes so cheap that all the remaining modes can be damped. In concrete terms, the ingredients of a multigrid technique are a fine-grid operator, a relaxation scheme, a restriction operator which interpolates a function from the fine grid to the coarse grid, a coarse-grid operator, and a prolongation operator interpolating a function from the coarse grid to the fine grid. The fine grid problem for the present example may be written

$$L^f U^f = F^f \quad (10)$$

Let V^f denote the fine-grid approximation. After the high-frequency content of the error $V^f - U^f$ has been sufficiently damped, attention shifts to the coarse grid. The coarse-grid problem is

$$L^c U^c = F^c \quad (11)$$

where

$$F^c = R [F^f - I^f V^f],$$

R being the restriction operator. After a satisfactory approximation V^c is obtained, the coarse-grid correction $(V^c - RV^f)$ is interpolated onto the fine grid by the prolongation operator P, yielding the corrected fine-grid solution

$$V^f \leftarrow V^f + P (V^c - RV^f) \quad (12)$$

The details of spectral multigrid techniques are furnished in [4]. Spectral multigrid techniques have been used to solve a variety of problems including the transonic full potential equation [5,6]. Additional applications of spectral methods to compressible flows are described in [7]. In the next section, we describe a multigrid algorithm for the incompressible Navier Stokes equations.

4. Navier Stokes Algorithms

This section is devoted to a description of recently developed algorithms for the simulation of instability and transition to turbulence in a flat-plate boundary layer. These algorithms deal with the primitive variable formulation of the Navier Stokes equations, and are based on the iterative methods discussed above in the simplest context. They are capable of handling geometric terms and variable viscosity.

The Navier Stokes equations in the so-called rotation form are

$$\begin{aligned} q_t &= q \times \omega + \nabla \cdot (\mu \nabla q) - \nabla P && \text{in } \Omega \\ \nabla \cdot q &= 0 && \text{in } \Omega \\ q(x,0) &= q_0(x) && \text{in } \Omega \end{aligned} \quad (13)$$

and

$$q = g \quad \text{on } \partial\Omega$$

where $q = (u,v,w)$ is the velocity vector, $\omega = \nabla \times q$ the vorticity, $P = p + 1/2 |q|^2$ the total pressure, μ the variable viscosity, Ω the interior of the domain, and $\partial\Omega$ its boundary. In the stability and transition problems under study, the domain Ω is cartesian and semi-infinite: periodic in the two horizontal directions (x,z) , and bounded by a wall at $y=0$. Fourier collocation can be used in the periodic directions (x,z) , and Chebyshev collocation is used in the vertical (y) direction. The collocation points in the periodic directions are given by a relation similar to Eq. (4). The vertical extent of the domain $0 < y < \infty$ is mapped onto $-1 < \xi < +1$. The velocities are defined and the momentum equations enforced at the points

$$\xi_j = \cos\left(\frac{\pi j}{N_y}\right), \quad j = 0, 1, \dots, N_y$$

The pressure is defined at the half points

$$\xi_{j+\frac{1}{2}} = \cos\left[\frac{\pi (j+1/2)}{N_y}\right], \quad j = 0, 1, \dots, N_y - 1$$

and the continuity equation is enforced at these points. The staggered grid avoids artificial pressure boundary conditions, and precludes spurious pressure modes.

After a Fourier transform in x and z , the temporal discretization (backward Euler for pressure, Crank-Nicolson for normal diffusion, and third or fourth-order Runge-Kutta for the remaining terms) of Eqs. (13) leads to

$$\begin{aligned} [I - MDM] Q + \Delta t A_0 \nabla \Pi &= Q_e \\ -A_x \nabla \cdot Q &= 0 \end{aligned} \quad (14)$$

where

$$\begin{aligned} Q &= \{\hat{q}_0^{n+1}, \hat{q}_1^{n+1}, \dots, \hat{q}_{N_y}^{n+1}\} \\ \Pi &= \{\hat{p}_{1/2}^{n+1}, \hat{p}_{3/2}^{n+1}, \dots, \hat{p}_{N-1/2}^{n+1}\} \\ \nabla &= \{ik_x, \frac{\partial}{\partial y}, ik_z\} \end{aligned} \quad (15)$$

M is the Chebyshev derivative operator, D the diagonal matrix with $1/2\mu\Delta t$ as its elements, and A_0 is the interpolation operator from the half points to cell faces, A_x vice versa. Obviously, the equations for each pair of horizontal wave number (k_x, k_z) are independent, and they can be written as the system

$$LX = F$$

where $X = [Q, \Pi]$. The iterative solution of this equation is carried out by preconditioning the system with a finite difference approximation on the Chebyshev grid, and applying a standard iterative technique such as Richardson, minimum residual or multigrid [8].

The method described above solves the implicit equations together as a set. The extension of this method to the more general cases of interest such as those involving two or more inhomogeneous directions is not straightforward. An alternative is the operator-splitting technique or the fractional step scheme [9]. This method yields implicit matrices which are positive definite and are easily amenable to iterative methods. In the first step, one solves the advection-diffusion equation

$$q_t^* = q^* \times \omega^* + \nabla \cdot (\mu \nabla q^*) \quad (16)$$

subject to the initial and boundary conditions

$$q^*(x, t_n) = q(x, t_n).$$

$$q^* = g^* \quad \text{on } \partial\Omega$$

Note that g^* has yet to be defined. In the second step, one solves for the pressure correction

$$q_i^{**} = \nabla P^{**} \quad (17)$$

$$\nabla \cdot q^{**} = 0$$

subject to the conditions

$$q^{**}(x,t^*) = q^*(x,t^*) \quad \text{in } \Omega$$

$$q^{**} \cdot \hat{n} = g \cdot \hat{n} \quad \text{in } \partial\Omega$$

where \hat{n} is the unit normal to the boundary. Further, the tangential component of the Eq. (17) holds on the boundary, i.e.,

$$q_i^{**} \cdot \hat{t} = -\nabla P^{**} \cdot \hat{t} \quad \text{in } \partial\Omega$$

where \hat{t} is a unit tangent vector to the boundary. Now g^* is defined [9] as (using Taylor expansion in t)

$$g^* \cdot \hat{n} = (g^n + \Delta t g_t^n) \cdot \hat{n}$$

$$g^* \cdot \hat{t} = [g^n + \Delta t (g_t^n + \nabla P^n)] \cdot \hat{t}.$$

Eq. (16) is discretized in the usual spectral collocation manner. After a temporal and spatial discretization of Eq. (17), the boundary conditions are built into the relevant matrix operators, and then a discrete divergence is taken. This results in a discrete Poisson equation (with as many algebraic equations as unknowns) for pressure, which can be solved by standard iterative techniques including the multigrid method.

5. Applications

These algorithms have been used to study the incipient stages of the transition process in channel flows [8] and parallel boundary layer flows [10]. Some representative results are provided here. The channel flow results pertain to the secondary instability associated with the so-called center modes. Unlike the Tollmien-Schlichting modes (sometimes alluded to as wall modes), the center modes always decay with a rather high decay rate. Their phase velocity is near unity and their maxima occurs near the center of the channel. The simulation had a Reynolds number of 5000 based on half-channel width, and the initial conditions consisted of a 20% amplitude two-dimensional center mode with two 1.5% amplitude skewed modes. The harmonic contents of the solution were monitored, and the grid was refined as deemed necessary. The finest grid was $144 \times 96 \times 108$. Plotted in Figure 3 are streamwise vorticity (left side) and spanwise vorticity (right side) contours on the streamwise planes at $x = 3/8, 7/16, 1/2$ and $9/16$ of the fundamental wavelength. The so-called peak plane would intersect these streamwise planes along a vertical line in the center of the frames. The structure of the vortex loop can be deduced from these plots. It differs in detail from that of the wall modes. The vortex structures are significant over only a small portion of the wavelength in the streamwise direction, whereas in the case of wall modes they cover almost the whole wavelength. Furthermore, the pinching of the vortex loop in the peak plane appears to be less acute in the case of the center modes. The harmonic history is displayed in Figure 4. The evolution of the secondary instability is apparent and it appears similar to that of the Tollmien-Schlichting modes. What is more interesting is the steep growth of the (0,2) and (2,2) modes which may lead to a strong tertiary instability. To resolve it in detail would require an even finer grid.

The parallel heated water boundary layer cases had a Reynold number of 1100 based on the displacement thickness, and the initial amplitudes of the two-dimensional and three-dimensional Tollmien-Schlichting waves were 2.7% and 0.4% respectively.

Three different situations were studied: 1) uncontrolled case, 2) heated fixed temperature case, and 3) heated active temperature case. In the heated fixed temperature case, the temperature was kept fixed at the initial value pertinent to the mean flow conditions, and the temperature evolution was totally neglected. In the heated active temperature case, the temperature evolution was taken into account by solving the temperature equation along with the momentum equations. In both the cases the wall temperature was 2.75% above the free stream temperature. Figures 5,6 and 7 display the harmonic histories. The fixed temperature case over-predicts the weakening effect of heating on the secondary instability. Figure 8 shows the spanwise vorticity contours on the peak plane. In the uncontrolled case (Figure 8 top left) a kink develops in the high-shear layer at time t equal to three Tollmien-Schlichting periods. It is generally accepted that a irrevocably quick succession of events follows thereafter leading to a turbulent spot formation. Heating the wall to 2.75% above the free stream temperature diffuses the high-shear layer as is obvious from Figure 8 (bottom left). However, within the subsequent one and one fourth period, turbulent spot formation appears to become imminent (Figure 8 top right). In the fixed temperature case, it is clear from Figure 8 (bottom right) that the high-shear layer formation is mellowed down even up to four and one fourth periods. This shows that the effect of temperature evolution is significant and deleterious in the nonlinear regime whereas it is quite negligible in the linear regime.

Acknowledgments

The assistance of D. L. Dwoyer, G. Erlebacher and T. A. Zang is appreciated.

References

1. Gottlieb, D., Orszag, S. A. 1977. "Numerical Analysis of Spectral Methods: Theory and Applications," CBMS-NSF Regional Conference Series in Applied Mathematics, SIAM.
2. Canuto, C., Hussaini, M. Y., Quarteroni, A., Zang, T. A. 1987. *Spectral Methods in Fluid Dynamics*, Springer Verlag.
3. Hussaini, M. Y., Zang, T. A. 1987. "Spectral methods in fluid dynamics," *Annual Review of Fluid Mechanics*, volume 19.
4. Zang, T. A., Wong, Y-S, Hussaini, M. Y. 1982. "Spectral multigrid methods for elliptic equations," *J. Comp. Phys.* 48:485-501 and 54:489-507.
5. Streett, C. L., Zang, T. A., Hussaini, M. Y. 1985. "Spectral multigrid methods with applications to transonic potential flow." *J. Comput. Phys.* 57:43,76.
6. Hussaini, M. Y., Salas, M. D., Zang, T. A. 1985. "Spectral methods for inviscid, compressible flows," *Advances in Computational Transonics*, pp.875-912, Habashi, W. G. (ed.), Pineridge Press, Swansea.
7. Hussaini, M. Y., Kopriva, D. A., Salas, M. D., Zang, T. A. 1985. "Spectral methods for Euler equations: Part 1. Fourier methods and shock-capturing," *AIAA J.* 23:64-70. "Part 2. Chebyshev methods and shock-fitting," *AIAA J.* 23:234-40.
8. Zang, T. A., Hussaini, M. Y., 1985. "Numerical Experiments on subcritical transition mechanisms," AIAA Paper No. 85-0296.

9. Zang, T. A., Hussaini, M. Y. 1986. "On spectral multigrid methods for time-dependent Navier-Stokes equations, *Appl. Math. Comp.*, to appear.
10. Zang, T. A., Hussaini, M. Y. 1985. "Numerical experiments on the stability of controlled shear flows," AIAA Paper No. 85-1698.

Table 1. Preconditioned Eigenvalues for One-dimensional First Derivative Model Problem

Preconditioning	Eigenvalues
Central Differences	$\frac{k\Delta x}{\sin(k\Delta x)}$
High Mode Cutoff	$\frac{k\Delta x}{\sin(k\Delta x)} \quad k\Delta x \leq (2\pi/3)$
	0 $(2\pi/3) < k\Delta x \leq \pi$
One-sided Differences	$e^{-i(k\Delta x/2)} \frac{k\Delta x/2}{\sin((k\Delta x)/2)}$
Staggered Grid	$\frac{(k\Delta x)/2}{\sin((k\Delta x)/2)}$

Table 2. Damping Factors for N = 64

p	Single-Grid	Multigrid
1	.9980	.9984
2	.9922	.9938
4	.9688	.9750
8	.8751	.9000
12	.7190	.7750
16	.5005	.6000
20	.2195	.3750
24	.1239	.1000
28	.5298	.2250
32	.9980	.6000

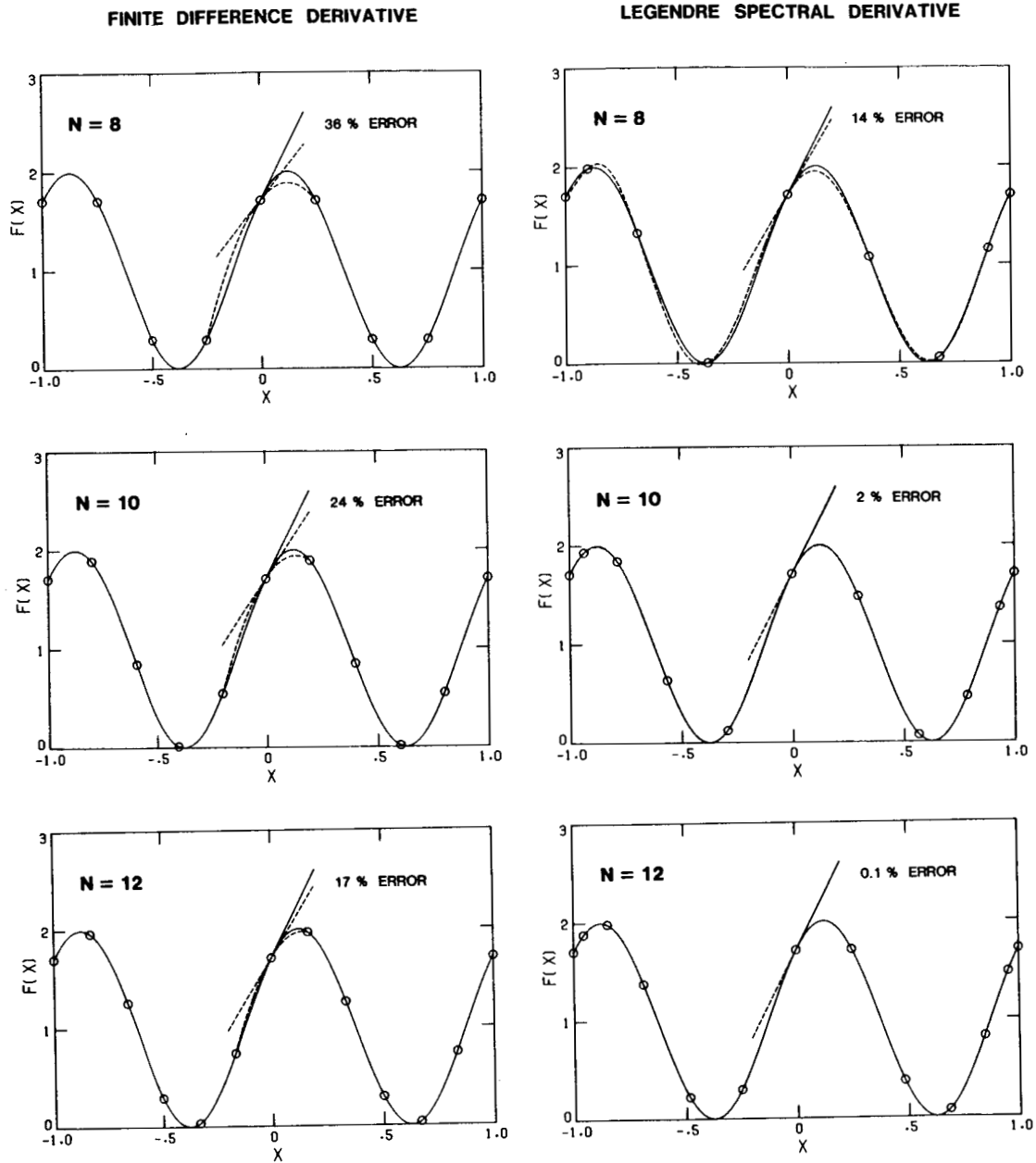


Figure 1: Comparison of finite difference (left) and Legendre spectral (right) differentiation. The solid curves represent the exact function and the dashed curves their numerical approximations. The solid lines are the exact tangents at $x = 0$ and the dashed lines the approximate tangents. The error in slope is noted as is the number of intervals N .

PERIODIC WAVE EQUATION

N: 32.

T: 6.2832

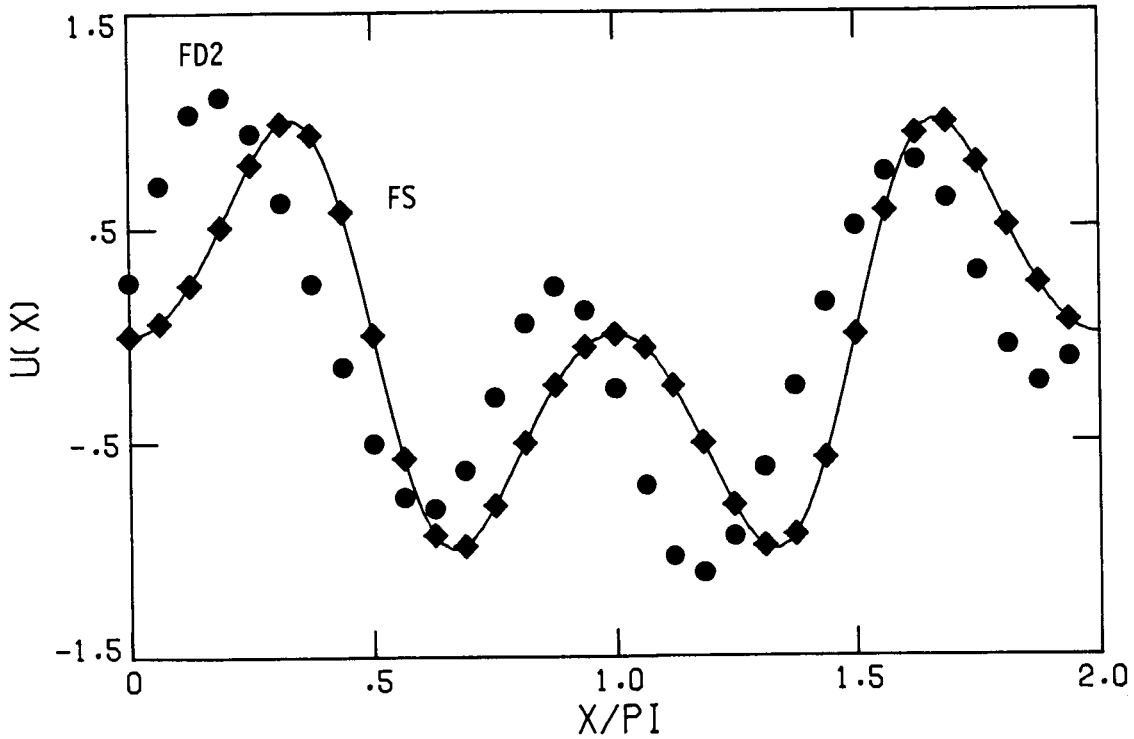


Figure 2: Finite difference (FD2) and Fourier spectral (FS) approximations after one period to a simple wave equation whose exact solution is represented by the curve.

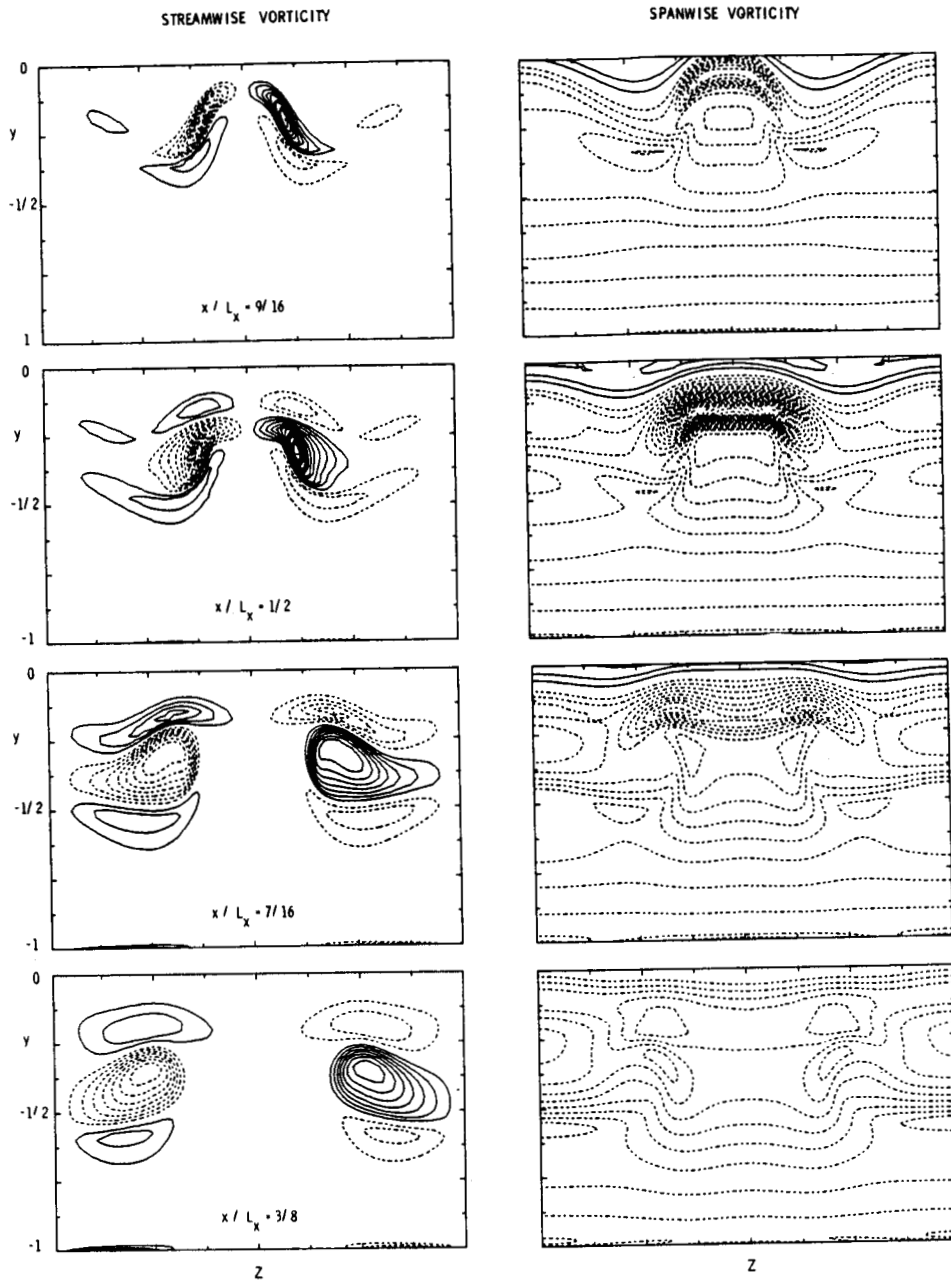


Figure 3: Streamwise (left) and spanwise (right) vorticity at four streamwise locations for a channel flow center mode transition. Only the lower half of the channel is shown.

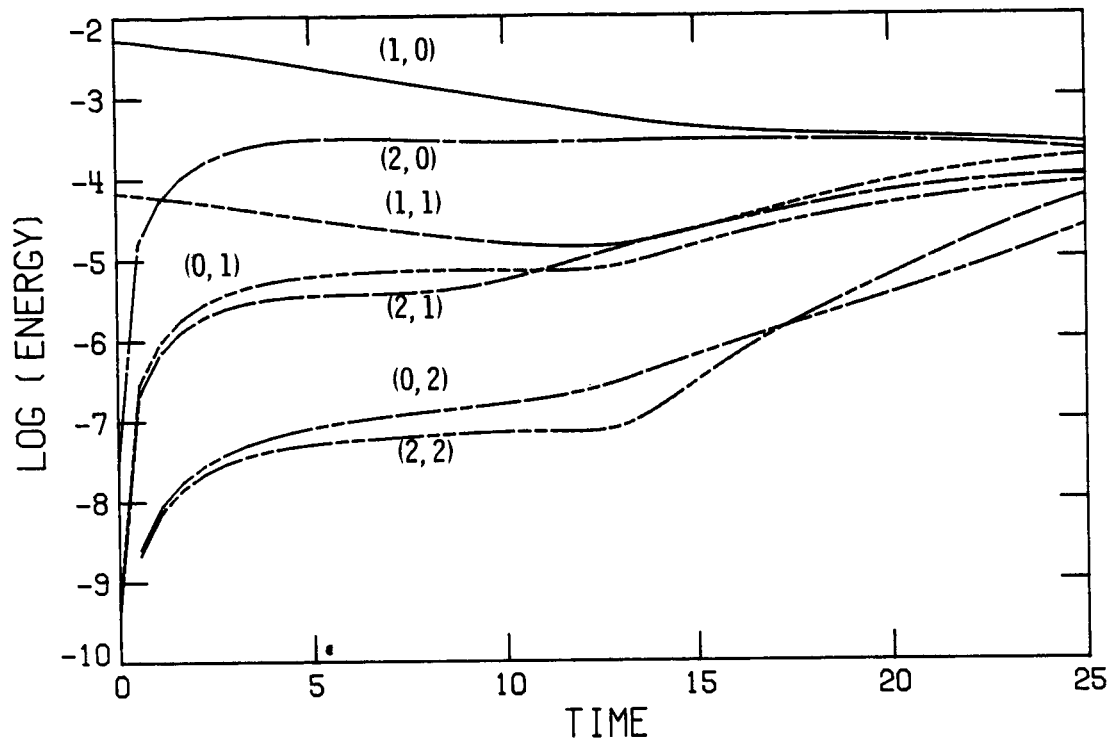


Figure 4: Harmonic history for a $Re = 5000$ center mode simulation.

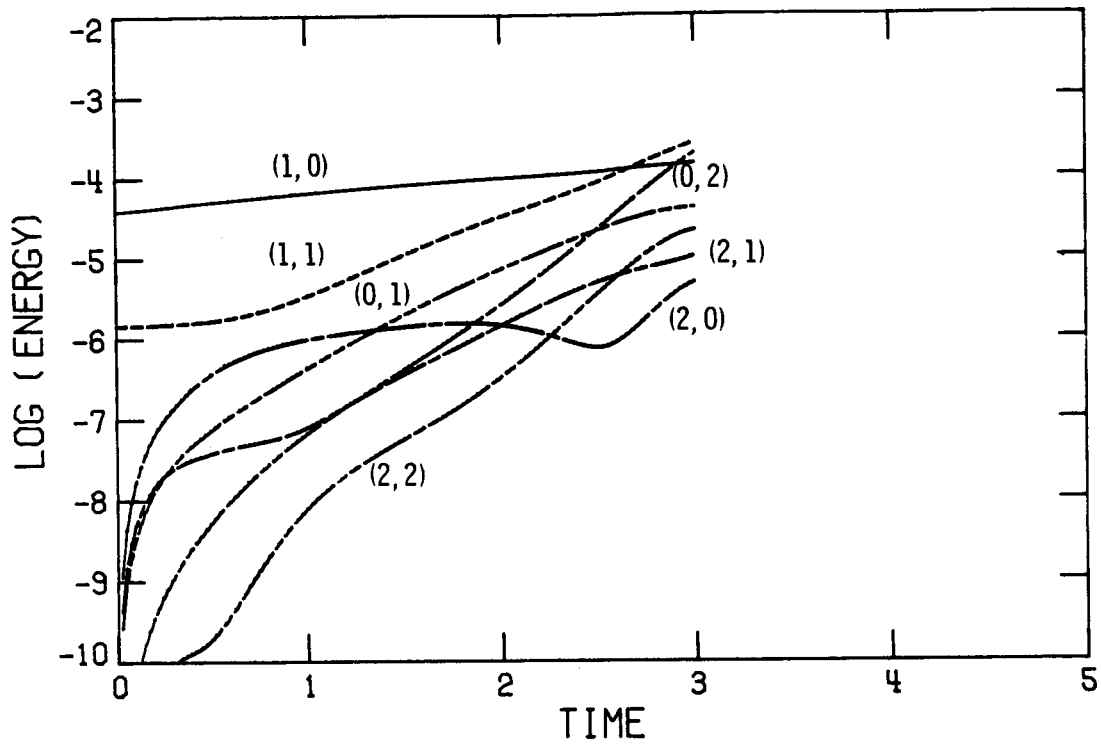


Figure 5: Harmonic history for a $Re = 1100$ boundary layer.

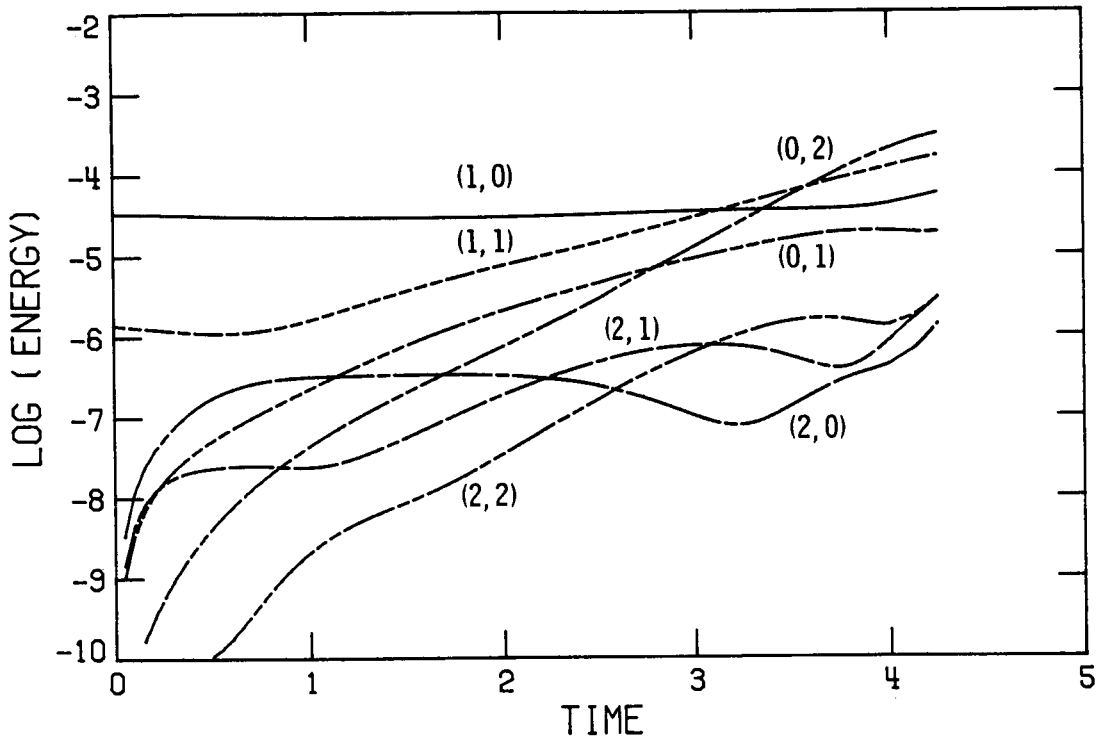


Figure 6: Harmonic history for a $Re = 1100$ heated boundary layer.

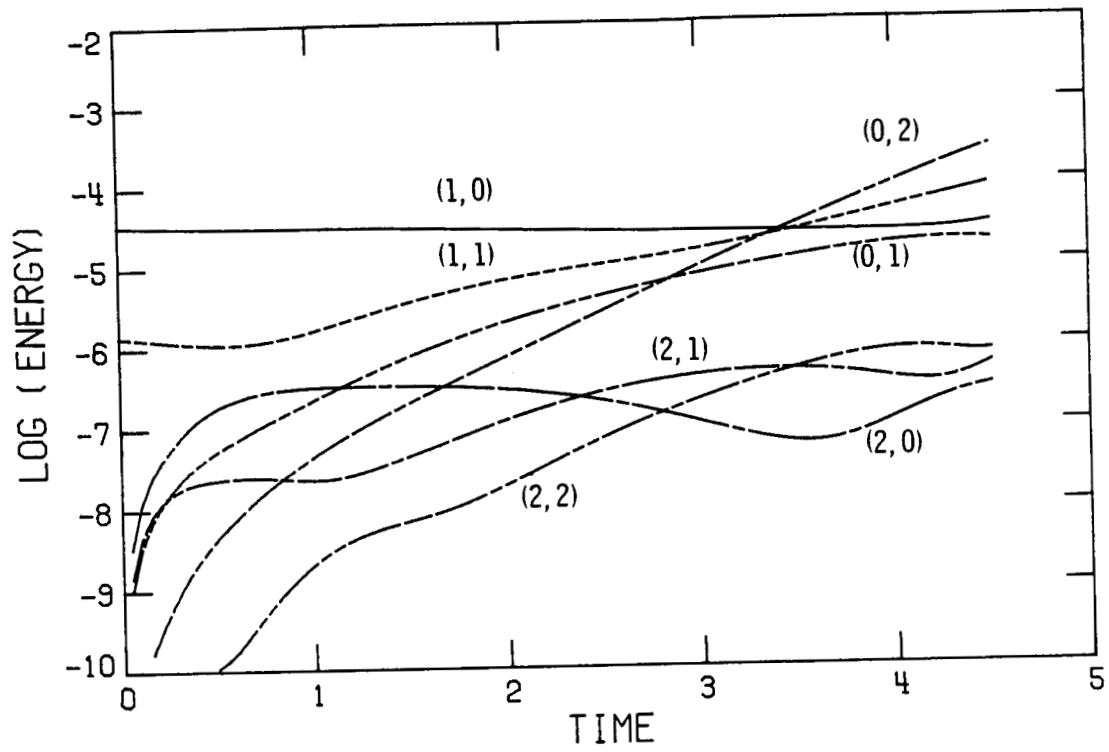


Figure 7: Same as Figure 6 but for fixed temperature.

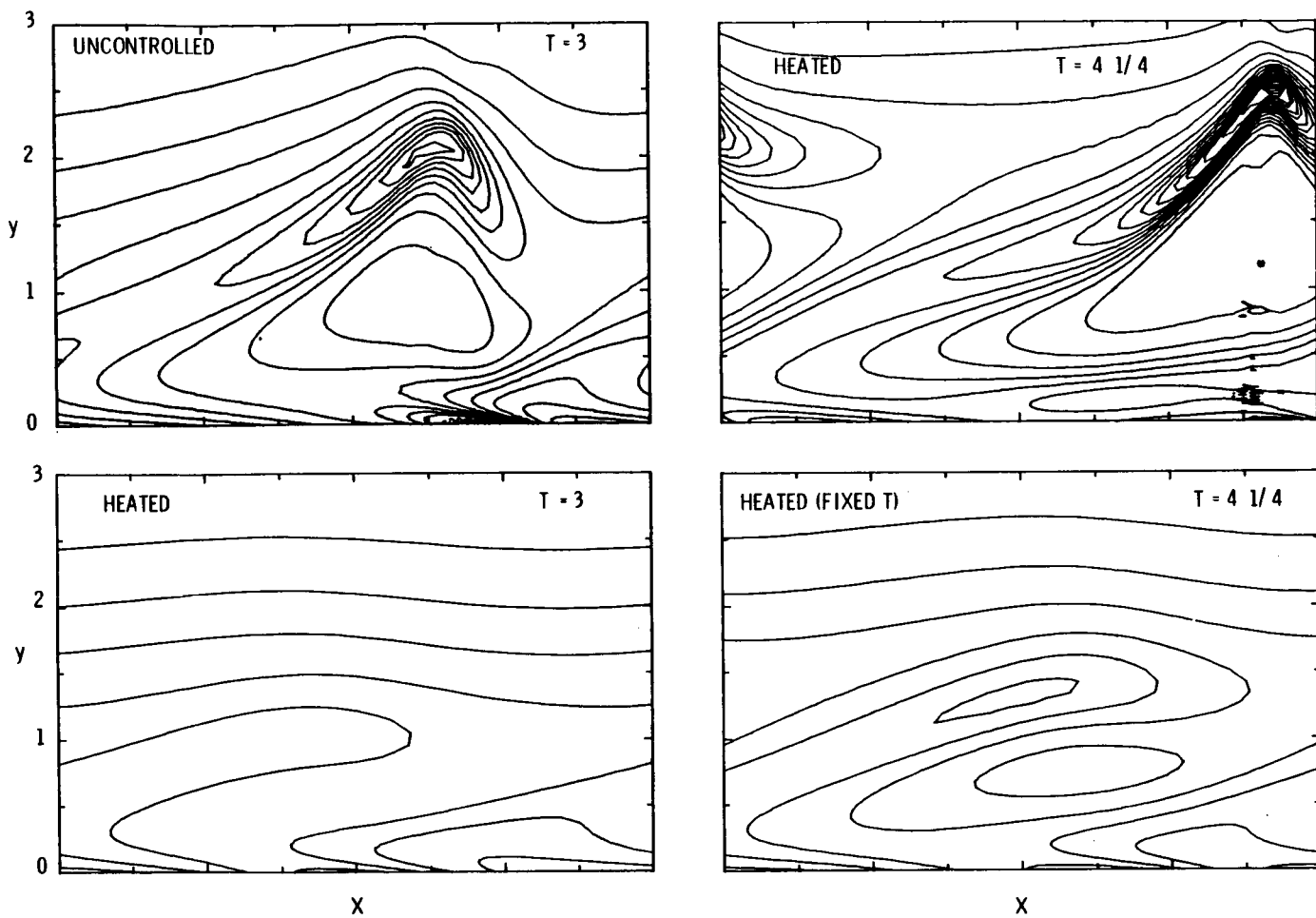


Figure 8: Vertical shear in the peak plane for $Re = 1100$ boundary layer simulation.

Standard Bibliographic Page

1. Report No. NASA CR-178178 ICASE Report No. 86-57		2. Government Accession No.		3. Recipient's Catalog No.	
4. Title and Subtitle SOME RECENT DEVELOPMENTS IN SPECTRAL METHODS				5. Report Date August 1986	
				6. Performing Organization Code	
7. Author(s) M. Y. Hussaini				8. Performing Organization Report No. 86-57	
9. Performing Organization Name and Address Institute for Computer Applications in Science and Engineering Mail Stop 132C, NASA Langley Research Center Hampton, VA 23665-5225				10. Work Unit No.	
				11. Contract or Grant No. NAS1-17070, NAS1-18107	
12. Sponsoring Agency Name and Address National Aeronautics and Space Administration Washington, D.C. 20546				13. Type of Report and Period Covered Contractor Report	
				14. Sponsoring Agency Code 505-90-21-01	
15. Supplementary Notes Langley Technical Monitor: Submitted to Proc. 10th Inter. J. C. South Conf. Num. Meth. in Fluid Dynamics Final Report					
16. Abstract This paper is solely devoted to spectral iterative methods including spectral multigrid methods. These techniques are explained with reference to simple model problems. Some Navier-Stokes algorithms based on these techniques are mentioned. Results on transition simulation using these algorithms are presented.					
17. Key Words (Suggested by Authors(s)) iterative spectral methods, stability and transition			18. Distribution Statement 34 - Fluid Mechanics and Heat Transfer 64 - Numerical Analysis Unclassified - unlimited		
19. Security Classif.(of this report) Unclassified		20. Security Classif.(of this page) Unclassified		21. No. of Pages 19	22. Price A02